



A Journal of



Accepted Article

Title: Analysis of Stability and (Anti)aromaticity of BN-Dibenzo[a,e]pentalenes

Authors: Milovan Stojanović and Marija Baranac-Stojanović

This manuscript has been accepted after peer review and appears as an Accepted Article online prior to editing, proofing, and formal publication of the final Version of Record (VoR). This work is currently citable by using the Digital Object Identifier (DOI) given below. The VoR will be published online in Early View as soon as possible and may be different to this Accepted Article as a result of editing. Readers should obtain the VoR from the journal website shown below when it is published to ensure accuracy of information. The authors are responsible for the content of this Accepted Article.

To be cited as: *Eur. J. Org. Chem.* 10.1002/ejoc.201801047

Link to VoR: <http://dx.doi.org/10.1002/ejoc.201801047>

Supported by



WILEY-VCH

Analysis of Stability and (Anti)aromaticity of BN-Dibenzo[a,e]pentalenes

Milovan Stojanović,^[b] and Marija Baranac-Stojanović^{*,[a]}

Abstract: Relatively scarce literature data on BN/CC isosterism in $4n\pi$ -electronic systems have prompted us to investigate theoretically the influence of BN pair position within the central butadiene fragment of dibenzo[a,e]pentalene on two fundamental molecular properties: stability and (anti)aromaticity. It was found that stability and aromaticity follow the same trend only for BN-orientational isomers. The source of different stability of other isomers was examined first by an analysis of bond types and their dissociation energies and then by isomerization energy decomposition analysis and was explained in terms of classical electrostatic interactions, quantum-mechanical orbital interactions, structural changes and electronic changes (transition from charge-separated π -system to the neutral one). (Anti)aromaticity was investigated by using three kinds of indices, HOMA, FLU_n and $NICS(1)_{zz}$, which indicated that delocalization at the central pentalene motif is almost unaffected by various BN arrangements, that of molecular perimeter is slightly affected, while the most affected subunits are five-membered rings and benzene-fused five-membered rings containing only one heteroatom.

Introduction

Pentalene is an unstable, 8π -electron antiaromatic hydrocarbon composed of two *ortho*-fused cyclopentadiene rings. Its stable derivatives can be obtained by formation of organometallic species,^[1] within non-IPR fullerenes,^[2] by introducing bulky substituents or by annulation to aromatic rings.^[3] This latter approach has led to compounds which are interesting for applications in organic electronics^[4] and as (anti)aromaticity probes,^[5] due to their intriguing electronic properties. Annulation of pentalene to two benzene rings gives rise to two isomers, dibenzo[a,e]pentalene and dibenzo[a,f]pentalene, both of which are known experimentally.^[6,7] The latter has been synthesized only recently, as mesityl derivative.^[7]

In recent years, the BN/CC isosterism has been widely exploited to tune physical properties and chemical reactivity of organic compounds.^[8] Hybrid BN/CC molecules have similar geometry as a parent hydrocarbon, but different electronic

structure. This is because the BN unit is isoelectronic to CC unit, but is polar. Thus, many BN analogues of hydrocarbons, mostly aromatic, were synthesized and applied in various fields, such as materials science,^[9] medicinal chemistry^[10] and synthetic chemistry.^[11] A number of theoretical and experimental studies done on BN-hydrocarbons have also enlarged our fundamental chemical knowledge.^[12]

It is interesting that polycycles with $4n\pi$ -electron molecular periphery have received little attention in the field of BN/CC isosterism. Recently, B_2N_2 analogues of benzopentalene^[13] and dibenzo[a,e]pentalene^[14] have been accessed experimentally. They proved to be stable with unique electronic structures. Thus, B_2N_2 -benzopentalene derivatives possess much larger HOMO-LUMO gap than the corresponding hydrocarbons.^[13] It was shown that different orientation of two BN units in the two isomeric B_2N_2 -dibenzopentalenes significantly affected (anti)aromaticity, optical and electronic properties.^[14] The latter work was followed by a detailed theoretical analysis of (anti)aromaticity of all three isomeric B_2N_2 -dibenzopentalenes, having BN units in the central butadiene fragment.^[15] Among the six possible isomers of BN-dibenzo[a,e]pentalene only one, containing borole and pyrrole moieties, was synthesized.^[16] Its borole ring was shown to be more antiaromatic than in dibenzoborole and in parent borole. Thus, it was concluded that unlike the conventional understanding that arene-annulation stabilizes borole ring by reducing antiaromaticity, the heteroarene-annulation enhances antiaromaticity of borole moiety in a molecule.^[16]

The fact that BN/CC isosterism is relatively unexplored in the area of antiaromatic compounds has prompted us to investigate theoretically all six isomeric BN-dibenzo[a,e]pentalenes (hereafter referred to as BN-dibenzopentalenes) having the BN pair in different positions within the central *trans*-butadiene fragment of dibenzopentalene structure. We aim to examine to what extent different BN positions widen the energy gap between the most and the least stable isomer. We then investigate whether the energy trend follows the trend of global, semilocal and local aromaticities. Since aromaticity and stability do not always go hand in hand, in cases in which their trend is not the same we aim to explain relative energies first by an analysis of bond types and their dissociation energies and then by performing the isomerization energy decomposition analysis, the details of which will be explained later in the text. Next, we explore the influence of BN position on local, semilocal and global (anti)aromaticity and compare it with (anti)aromaticity of the parent hydrocarbon, dibenzopentalene, as well as with other individual structures that appear as substructures in BN-dibenzopentalene isomers.

Computational Details

All calculations were done at the B3LYP/6-311+G(d,p) level of theory.^[17] Molecular structures were optimized by employing Gaussian 09 program package.^[18] When stability calculation

[a] Prof. Dr. M. Baranac-Stojanović
University of Belgrade – Faculty of Chemistry
Studentski trg 12-16
11000 Belgrade, Serbia
E-mail: mbaranac@chem.bg.ac.rs
www.chem.bg.ac.rs/osoblje/48-en.html

[b] Dr. Milovan Stojanović
University of Belgrade
Institute of Chemistry, Technology and Metallurgy
Center for Chemistry
Njegoševa 12
11000 Belgrade, Serbia

Supporting information for this article is given via a link at the end of the document.

indicated an internal instability of the wave function, optimization was repeated for open-shell singlet at the UB3LYP/6-311+G(d,p) level. Vibrational analysis confirmed that the obtained structures were energy minima, as they had no imaginary frequencies. For (anti)aromaticity studies we used three indices which belong to three different manifestations of the phenomena: the structural HOMA index,^[19] the electronic FLU_{π} index^[20] and the magnetic $NICS(1)_{zz}$ index.^[21] The harmonic oscillator model of aromaticity (HOMA) index is based on equalization of bond lengths in aromatic species. Its positive values close to one indicate aromaticity, negative values denote antiaromaticity and values close to zero refer to nonaromaticity. For HOMA calculations we used the following α/R_{opt} (Å): 118.618/1.4386 (BC), 72.03/1.402 (BN), 257.7/1.388 (CC) and 93.52/1.334 (CN).^[19a] The aromatic π fluctuation (FLU_{π}) index describes the fluctuation of π -electronic charge between adjacent atoms in a given ring. This index is close to zero in aromatic compounds and differs from it in nonaromatic and antiaromatic species. The HOMA and FLU_{π} indices can be used for any circuit in a molecule. They were calculated by using the Multiwfn program.^[22] The nucleus independent chemical shift ($NICS(1)_{zz}$) index measures the out of plane component of magnetic shielding at a point located 1 Å above the center of a given ring. The shielding values were calculated by employing the GIAO approach.^[23] Significantly negative and positive NICS values denote aromaticity and antiaromaticity, respectively, and values close to zero indicate nonaromaticity. Gaussian 09 was used for NICS calculations. The localized molecular orbital energy decomposition analysis (LMOEDA)^[24] was performed by using the Gamess program package.^[25] Some of the original labels for various energy components^[24] were changed in this work. Thus, ΔE_{poi} is labeled, herein, as ΔE_{oi} (orbital interaction energy). The exchange (ΔE_{ex}) and repulsion energy (ΔE_{rep}) were summed up to represent the Pauli repulsion energy (ΔE_{Pauli}).

The only experimentally known compound is a derivative of **1,4** isomer of BN-dibenzopentalene.^[16] The calculated molecular structure was very similar to the experimentally obtained one: selected bond lengths deviated from each other by less than 0.02 Å and bond angles by less than 1.4°. Some deviations were expected, because experimental data are from X-ray analysis of B,N-disubstituted derivative (see, Table S1 in the Supporting Information).

Results and Discussion

Structure and stability analysis

The six isomers of BN-dibenzopentalene are labeled according to the position of heteroatoms within the central *trans*-butadiene fragment of the parent hydrocarbon, as is shown in Figure 1. For example, **1,2** isomer contains nitrogen atom at position 1 and boron atom at position 2, while its BN-orientational **2,1** isomer has the opposite arrangement of heteroatoms. This is visible in Figure 2, which represents the optimized structures of dibenzopentalene and its six BN isomers, along with their bond lengths and relative energies.

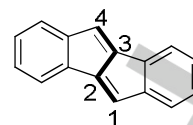


Figure 1. Numbering of the central conjugated diene moiety used to label the six isomeric BN-dibenzopentalenes.

As the results from Figure 2 show, there is a large difference in energy between the least (**1,3**) and the most stable isomer (**2,1**) which amounts 51.82 kcal/mol. In the analysis of the obtained energy trend, we first discuss the π -electronic changes within the butadiene moiety of dibenzopentalene that take place upon CC \rightarrow BN substitution. The BN unit which is isoelectronic with the CC double bond is shown in Figure 3. Therefore, replacement of a single CC double bond of the central conjugated diene moiety in dibenzopentalene with the BN pair (1,2-substitution), or replacement of terminal carbon atoms (1,4-substitution) can retain the neutral π -electronic system. However, replacement of two internal carbon atoms (2,3-substitution) or one internal and one terminal atom (1,3-substitution) creates a charge separation within the π -system of the central butadiene moiety (Figure 3). Our calculations on BN-substituted *trans*-butadiene^[26] show that the energy trend of BN-dibenzopentalenes is not determined by the stability of this fragment in the molecule, nor it is determined by the stability of the BN-substituted central pentalene motif (Figure S1 in the Supporting Information). Clearly, energetic stability is affected by additional benzene rings. Thus, in the case of 1,3-substitution, it is possible to obtain the neutral π -system if one benzene ring loses its aromatic π -electronic sextet and adopts an *ortho*-quinoidal structure (Figure 3). However, 2,3-substitution inevitably results in charge separated π -electronic system, but **2,3** isomer is not the least stable.

The structural data from Figure 2 suggest that **3,1** isomer escapes destabilization due to separated charges by adopting an isoindole substructure and, in this way, it forms the neutral π -system (Figure 4). Thus, benzene ring of isoindole substructure has only two short bonds (1.377 Å and 1.379 Å) and this contrasts the pattern of bond length alternation of benzene in the parent dibenzopentalene which has three short bonds (1.384 Å, 1.387 Å and 1.392 Å). The two exocyclic CC bonds in **3,1** (1.409 Å and 1.416 Å) are shorter than the corresponding bonds in dibenzopentalene (1.477 Å and 1.464 Å), as well.

Its orientational **1,3**-isomer, however, does not escape charge separation of the π -system, which is evident from the analysis of bond lengths given in Figure 2. Thus, benzene ring, which is fused to borole, contains three shorter bonds (1.376-1.381 Å) and three longer bonds (1.417-1.437 Å). The two exocyclic CC bonds are longer (1.461 Å and 1.496 Å) than in **3,1** (1.409 Å and 1.416 Å) and the BC and CN bonds are short (1.464 Å and 1.318 Å, respectively). Obviously, there is no

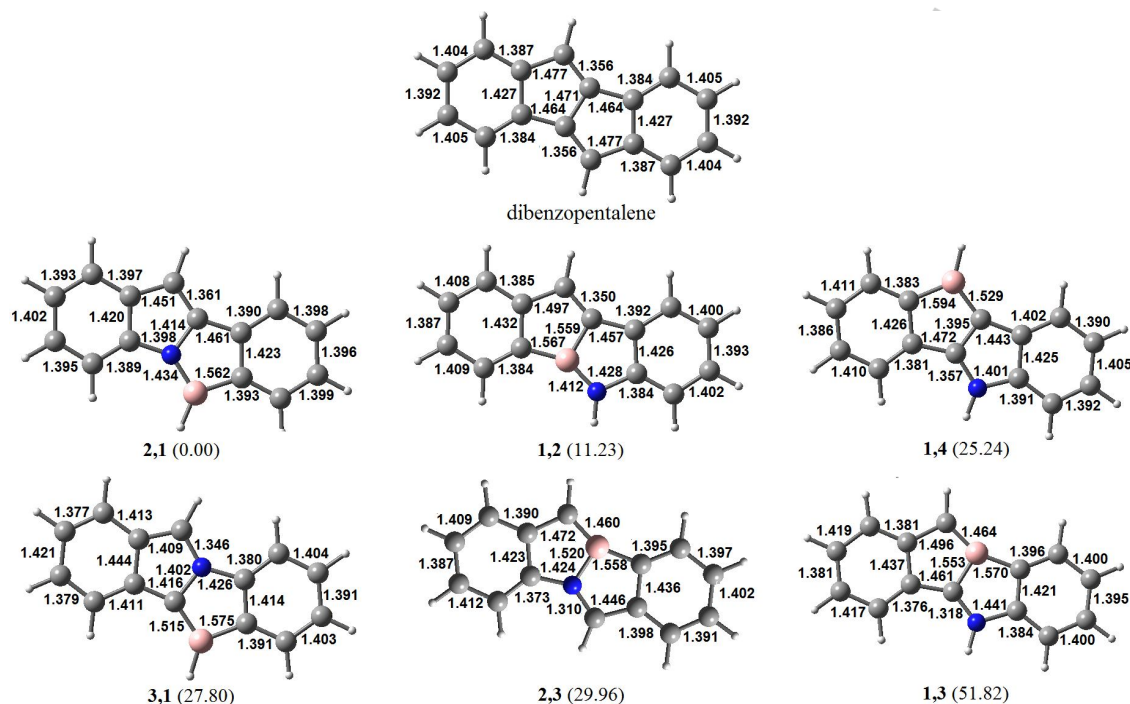


Figure 2. Optimized structures (B3LYP/6-311+G(d,p)) of dibenzopentalene and its six isomeric BN analogues, along with their bond lengths (in Å) and relative energies (in kcal/mol).

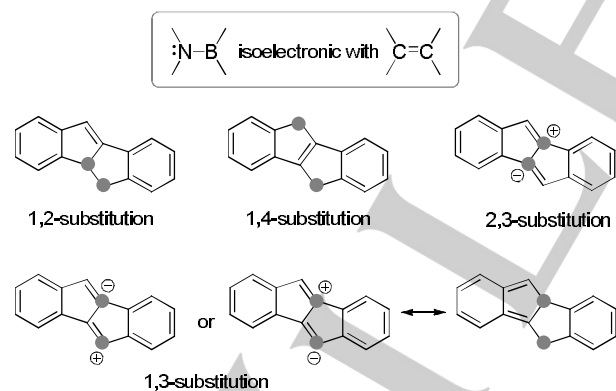


Figure 3. Substitution of various CC units within the central conjugated diene fragment of dibenzopentalene with the isoelectronic BN pair.

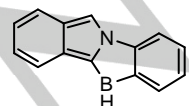


Figure 4. The main resonance form of 3,1 isomer of BN-dibenzopentalene.

tendency for the formation of 8 π -electron benzo[c]borole substructure. The 1,3 isomer was optimized as closed-shell, charge-separated form and as open-shell singlet and the latter was found to be only slightly lower in energy ($\Delta E_{OS-CS} = -0.01$ kcal/mol and $\Delta G_{OS-CS} = -0.63$ kcal/mol) with negligible changes in geometry. This means that diradical character would not be pronounced and that charge-separated structure is more probable for this isomer (Figure 5).^[27] The calculated Hirshfeld charges,^[28] given in Table 1, are in accordance with charge separation. Thus, the C–N fragment takes up positive charge (C/N 0.040/–0.035) and the B–C moiety negative charge (C/B –0.157/0.018). We anticipate that chemical reactivity of 1,3 will be affected by this charge distribution which makes C2 electrophilic and C4 nucleophilic.

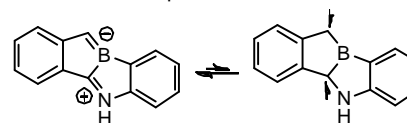
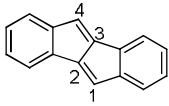
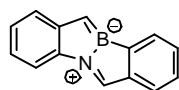


Figure 5. Charge-separated and open-shell singlet structures of 1,3 isomer of BN-dibenzopentalene.

Table 1. Calculated Hirshfeld charges of the atoms that constitute the central conjugated diene fragment.


Position	Hirshfeld charge/atom			
	1	2	3	4
dibenzopentalene	-0.027/C	-0.016/C	-0.016/C	-0.027/C
1,2	-0.191/N	0.180/B	-0.101/C	-0.016/C
2,1	0.189/B	-0.134/N	0.045/C	-0.058/C
2,3	0.094/C	-0.076/N	0.070/B	-0.170/C
1,3	-0.035/N	0.040/C	0.018/B	-0.157/C
3,1	0.120/B	-0.090/C	-0.008/N	0.020/C
1,4	-0.072/N	0.072/C	-0.147/C	0.151/B

The charge separation of **2,3** isomer (Figure 6) is clearly visible from the large negative/small positive charge at C/B which are $-0.170/0.070$ and large positive/small negative charge at C/N which are $0.094/-0.076$ (Table 1). The two carbon atoms in **2,3** have the highest positive and negative charges, which should make them as highly electrophilic and nucleophilic. Furthermore, the CN and BC bonds are the shortest in this isomer, 1.310 \AA and 1.460 \AA , respectively. The existence of separated charges is certainly the reason for the high energy of this isomer ($E_{\text{rel}} = 29.96 \text{ kcal/mol}$), but it is by 21.86 kcal/mol more stable than **1,3** isomer and by only 2.16 kcal/mol less stable than **3,1** isomer.

**Figure 6.** Charge-separated structure of **2,3** isomer of BN-dibenzopentalene.

Stability and aromaticity

An analysis of relative energies in Figure 2 shows that among the BN-orientational isomers **2,1** is more stable than **1,2** (11.23 kcal/mol) and **3,1** is more stable than **1,3** (24.02 kcal/mol).

An intuitive explanation of greater stability of **2,1** vs **1,2** can be based on the existence of 10π -electron indole substructure in **2,1** vs the 8π -electron benzo[*b*]borole subunit in **1,2**. Indeed, our (anti)aromaticity calculations, given in Figure 7, show that indole moiety in **2,1** is aromatic, while benzoborole moiety in **1,2** is nonaromatic. In addition, the other subunits, azaborolidine and benzene, are similarly nonaromatic and aromatic, respectively, in the two isomers. Within indole/benzoborole moieties, benzene is more aromatic in the more stable **2,1** isomer, pyrrole in **2,1** is very weakly aromatic while borole in **1,2** is antiaromatic. The perimeter of the whole molecule is slightly more delocalized in **2,1** isomer. Hence, relative stability of **1,2/2,1** isomeric pair is

well accounted for by (anti)aromaticity considerations at all levels (individual rings, benzene-fused five-membered rings and perimeter of molecule).

Similarly, the relative stability of another isomeric pair, **3,1** and **1,3**, can be explained by taking into account two factors: formation of an almost neutral π -electronic system in the more stable **3,1** and its higher aromaticity content. For the former, it should be noted that a small contribution of separated charges is possible, since Hirshfeld charges (Table 1) indicate slightly increased negative charge at the B–C fragment (B/C $0.120/-0.090$) and positive charge at the C–N fragment (N/C $-0.008/0.020$); very small negative charge on nitrogen should be due to its involvement in the 6π -electron pyrrole moiety, which is more delocalized than pyrrole ring in indole (Figure 7). As for the aromaticity, we point out the following. The more stable **3,1** contains aromatic isoindole moiety, while the less stable **1,3** has nonaromatic benzo[*c*]borole moiety. The azaborolidine moiety is nonaromatic in both isomers and benzene fused to it is similarly aromatic in the two isomers. The large difference between the isomers is that the more stable **3,1** possesses aromatic pyrrole ring, while the less stable **1,3** contains an antiaromatic borole ring. If a conclusion is to be drawn on the basis of both HOMA and FLU_{π} , the perimeter of **3,1** is aromatic and that of **1,3** very weakly aromatic.

However, (anti)aromaticity considerations do not explain relative stability of other isomers (the details are given in the Section S1 in the Supporting Information), so that in the next section we discuss bond dissociation energies (BDEs) and stability trend.

Stability trend and bond dissociation energies

The four isomers having the neutral π -system are more stable than the two charge-separated isomers (Figure 2). In the former group, the most stable members, **2,1** and **1,2**, have direct B–N connection. This result agrees with previous observations for aromatic BN systems,^[12c,29] as well as for BN analogues of antiaromatic cyclobutadiene,^[30] that isomers containing B–N bond or B–N–B–N linkage are the most stable ones.

Upon going from **2,1** to **1,4** (25.24 kcal/mol) the molecule loses B–N bond, $\text{BDE} = 144.4 \text{ kcal/mol}$ ($139.7 \text{ kcal/mol}^{[31]}$), calculated for aminoborane, and forms B–C bond, $\text{BDE} = 117.8 \text{ kcal/mol}$, calculated for vinylborane. Thus, their relative energy is well accounted for by this difference. If we start from **1,2** and form **1,4** (14.01 kcal) the B–N bond is replaced with the C–N bond, $\text{BDE} = 104.0 \text{ kcal/mol}$, calculated for vinylamine. This points to the weaker stability of **1,4**, but overestimates the energy difference.

Further isomerization of **1,4** into **3,1** (2.56 kcal/mol) results in the loss of one C–C bond, $\text{BDE} = 112.6 \text{ kcal/mol}$, calculated for styrene, and formation of one C–N bond. This correctly points to the lower stability of **3,1**, though does not fully account for the energy difference, which is smaller than the difference in the bond strengths.

Formation of **2,3** from **3,1** (2.16 kcal) leads to the loss of the C–N bond and formation of the strong B–N bond, but also leads to the charge separation of the π -electronic system, which

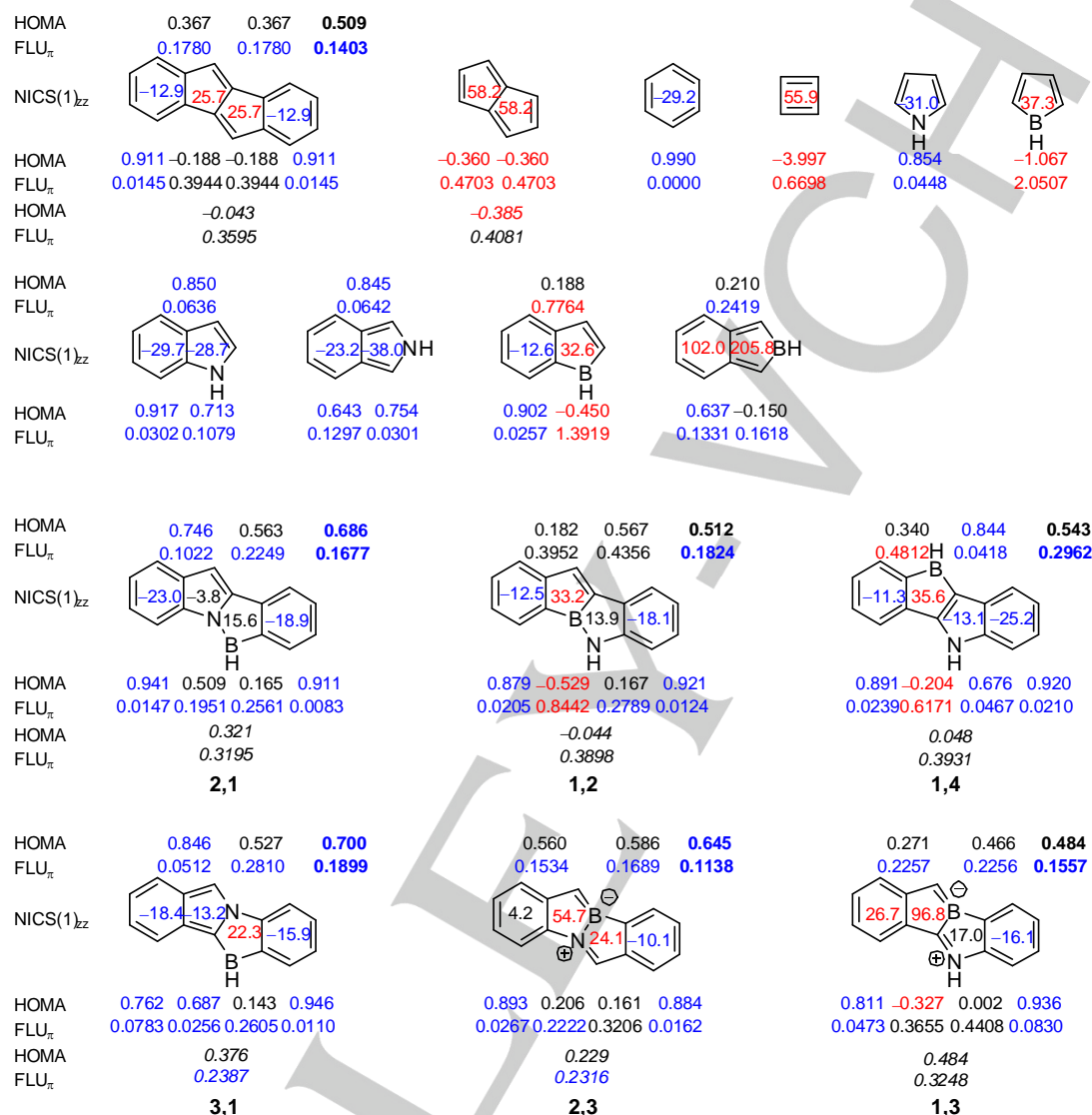


Figure 7. HOMA, FLU_π and NICS(1)_{zz} values for dibenzopentalene and its BN-substituted analogues (benzene, cyclobutadiene, pyrrole, borole, indole, isoindole, benzo[*b*]borole and benzo[*c*]borole are also included for comparison). NICS(1)_{zz} data are given inside the rings. HOMA and FLU_π data, which are shown below the structures, correspond to individual rings and to the central pentalene moiety (values in italic) and those which are given above the structures refer to the two benzene-fused five-membered rings and to the perimeter of a molecule (values in bold). Blue-coloured values indicate aromaticity, red-coloured ones denote antiaromaticity and those given in black describe nonaromatic system, or are at the borderline between (anti)aromaticity and nonaromaticity.

destabilizes the molecule. Finally, upon going from **2,3** to **1,3** (21.86 kcal/mol) the charge-separation remains while the strong B–N bond is replaced with the weaker B–C bond and this well accounts for their energy difference.

To get more detailed insight into the individual effects which determine the stability trend of the studied compounds, in the next section we discuss results from the isomerization energy decomposition analysis (IEDA).^[32]

Isomerization energy decomposition analysis

We begin with the analysis of relative stability of **1,4** isomer and **2,1/1,2** isomeric pair. The **1,4** isomer can be formed from both **2,1** and **1,2** by rotating the (indole – H) or (benzo[*b*]borole – H) subunits, respectively, by 180°, as is shown in Table 2. This isomerization energy (ΔE_{iso}) can be decomposed into two main parts, that is, the change in deformation energy ($\Delta\Delta E_{\text{def}}$) and the

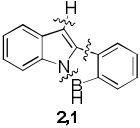
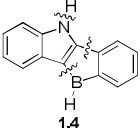
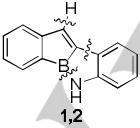
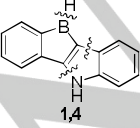
change in interaction energy ($\Delta\Delta E_{\text{int}}$): $\Delta E_{\text{iso}} = \Delta\Delta E_{\text{def}} + \Delta\Delta E_{\text{int}}$. The first one reflects energy changes due to structural changes occurring during the isomerization and the second one is associated with energy changes due to changes in chemical bonds. In the performed analysis, we homolytically broke B–N and C–H bonds in **2,1**/**1,2** and also the C–C bond around which rotation took place, so that we obtained three interacting fragments for each case: a hydrogen radical for both isomerizations, $\text{C}_8\text{H}_4\text{N}$ triradical and $\text{C}_6\text{H}_5\text{B}$ diradical for **2,1** \rightarrow **1,4** isomerization and $\text{C}_8\text{H}_4\text{B}$ triradical and $\text{C}_6\text{H}_5\text{N}$ diradical for **1,2** \rightarrow **1,4** isomerization. All unpaired electrons within one fragment had the same spin, while fragments which interacted with one another had opposite spin electrons, so that they could form bonds. Deformation energy (ΔE_{def}) of each fragment (except hydrogen radical) was calculated as energy difference between its geometry in the studied molecules and its optimal geometry. The decomposition of ΔE_{iso} into $\Delta\Delta E_{\text{def}}$ and $\Delta\Delta E_{\text{int}}$ (Table 2) shows that the major cause of energy gain upon formation of **1,4** from both **2,1** and **1,2** is ΔE_{int} , 98% and 72%, respectively (the rest comes from ΔE_{def}).

To get a deeper insight into the factors responsible for weaker bonding in **1,4** we decomposed the $\Delta\Delta E_{\text{int}}$ term into four physically meaningful energy components: change in the strength of classical electrostatic interactions ($\Delta\Delta E_{\text{elstat}}$) involving

attractive (electron-nucleus) and repulsive (electron-electron and nucleus-nucleus) forces, change in quantum-mechanical orbital interactions which include destabilizing Pauli interactions ($\Delta\Delta E_{\text{Pauli}}$) and stabilizing interactions ($\Delta\Delta E_{\text{oi}}$) related to the bond formation, charge transfer (donor-acceptor interactions between occupied orbitals of one fragment with empty orbitals of another) and polarization (empty-occupied orbital mixing within one fragment due to presence of another one), and change in dispersion energy ($\Delta\Delta E_{\text{disp}}$). The magnitudes of each energy component between fragments of one molecule (ΔE values in Table 2) were calculated by means of LMOEDA.^[24]

The results show that **1,4** isomer suffers from Pauli destabilization relative to both **2,1** and **1,2** (almost double for the latter), and from weaker electrostatic attraction with respect to **2,1**. Stabilizing orbital interactions are more intense in **1,4** relative to both starting isomers, while contribution from dispersion energy is small. When **2,1** isomerizes into **1,4** the main part of increased Pauli repulsion is cancelled by the more favourable orbital interaction, so that ~80% of energy rise comes from weaker electrostatic forces. This can be mainly attributed to the change from partially ionic B–N bond^[31] to the long B–C bond (1.529 Å, Figure 2) and to the ~0.01 Å increase in the C–C bond which weakens its electrostatic component. Increase in the Pauli repulsion can be ascribed to the change in the relative spatial

Table 2. Contribution of various energy components to the total binding interactions between three fragments in the studied BN analogues of dibenzopentalene and energy changes (values in bold) occurring upon constitutional isomerization.^[a] Values are in kcal/mol, calculated at the UB3LYP/6-311+G(d,p) level.

Molecule	ΔE_{tot}	ΔE_{def}	ΔE_{int}	ΔE_{elstat}	ΔE_{Pauli}	ΔE_{oi}	ΔE_{disp}	Interacting fragments ^[b]
	ΔE_{iso}	$\Delta\Delta E_{\text{def}}$	$\Delta\Delta E_{\text{int}}$	$\Delta\Delta E_{\text{elstat}}$	$\Delta\Delta E_{\text{Pauli}}$	$\Delta\Delta E_{\text{oi}}$	$\Delta\Delta E_{\text{disp}}$	
 2,1	-339.75	45.09	-384.84	-325.30	540.90	-533.49	-66.95	H(d) C ₆ H ₅ B(t) C ₈ H ₄ N(q)
 1,4	-314.50	45.53	-360.03	-305.67	709.97	-697.32	-67.01	H(d) C ₆ H ₅ B(t) C ₈ H ₄ N(q)
2,1 \rightarrow 1,4	25.25	0.44	24.81	19.63	169.07	-163.83	-0.06	
 1,2	-356.46	22.60	-379.06	-356.43	571.76	-526.37	-68.02	H(d) C ₆ H ₅ N(t) C ₈ H ₄ B(q)
 1,4	-342.45	26.53	-368.98	-416.07	886.77	-772.28	-67.40	H(d) C ₆ H ₅ N(t) C ₈ H ₄ B(q)
1,2 \rightarrow 1,4	14.01	3.93	10.08	-59.64	315.01	-245.91	0.62	

[a] ΔE_{tot} = total binding energy between three fragments, ΔE_{def} = deformation energy, ΔE_{int} = interaction energy, ΔE_{elstat} = electrostatic energy, ΔE_{Pauli} = Pauli repulsion, ΔE_{oi} = orbital interaction energy, ΔE_{disp} = dispersion energy, ΔE_{iso} = isomerization energy. [b] Interacting fragments involved in ΔE_{int} energy: d (doublet), t (triplet), q (quartet).

orientation of indole and benzene ring, so that the π -electron rich part of indole comes closer to benzene's π -electrons in **1,4**. In the case of **1,2** \rightarrow **1,4** isomerization, apart from an increase in Pauli repulsion due to the change in spatial orientation between benzo[*b*]borole and benzene, there is an additional factor, $N_{LP}-CC_{\pi}$ interaction, which contributes to larger overall repulsion, which is almost the sole factor contributing to the increase in $\Delta\Delta E_{int}$.

The calculated Hirshfeld charges, shown in Table 1, indicate the π -electron delocalization over the central four-atomic fragment in **1,4** (Figure 8). Thus, nitrogen atom in **1,4** is less negatively charged than nitrogen atoms in **1,2/2,1** isomers (-0.072 in **1,4** and $-0.191/-0.134$ in **1,2/2,1**), while C3 is more negatively charged (-0.147 in **1,4** and $-0.101/0.045$ in **1,2/2,1**). Boron atom in **1,4** is also less positive than boron atoms in **1,2/2,1** (0.151 in **1,4** and $0.180/0.189$ in **1,2/2,1**). This delocalization is reminiscent of mostly one-directional π -electron delocalization of push-pull alkenes^[33] and can affect chemical reactivity of **1,4** by making C2 as electrophilic and C3 as nucleophilic.

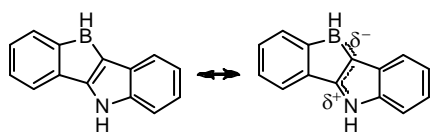


Figure 8. The π -electron delocalization from nitrogen to boron in **1,4** isomer of BN-dibenzopentalene.

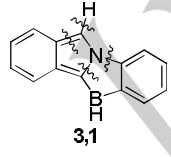
To search for the origin of just slightly higher energy of **3,1** relative to **1,4** isomer we have studied contributions of various

energy components to the **1,4** \rightarrow **3,1** isomerization energy. The isomerization was carried out by rotating the C–N unit in its sextet electronic state (Table 3). The results show that the slightly greater energy content of **3,1** comes exclusively from deformation energy, which can be ascribed to the transition of benzene structure into the *ortho*-quinoidal one.

Next, we examine the energy trend of **3,1** ($E_{rel} = 27.80$ kcal/mol), **2,3** ($E_{rel} = 29.96$ kcal/mol) and **1,3** ($E_{rel} = 51.82$ kcal/mol) isomers. The applied isomerization scheme is the following. The **2,3** isomer can give rise to both **3,1** and **1,3** if the BC or CN fragments, respectively, are rotated by 180° (Table 4). Thus, to study the origin of isomerization energy (ΔE_{iso}) we have homolytically broken all four bonds around these fragments, as is shown by formulas in Table 4. When **2,3** isomerizes into the slightly more stable **3,1** there is a drop in deformation energy component, which, now, includes changes in both geometry and in electronic structure. The latter is associated with transformation from the charge-separated to the neutral π -system. The $\Delta\Delta E_{def} = -19.88$ kcal/mol is the only factor responsible for energy loss upon isomerization and is counteracted by the large increase in $\Delta\Delta E_{int} = 17.79$ kcal/mol, that is, by formation of weaker bonds. As the results in Table 4 show, stronger bonding in the less stable **2,3** is almost equally caused by electrostatic attraction and stabilizing orbital interactions, 54% and 46%, respectively. Thus, the charge-separation of the π -system in **2,3** acts in two opposite directions: it destabilizes π -electronic structure, but strengthens the electrostatic component of chemical bonds.

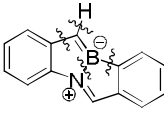
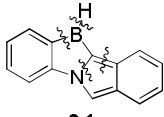
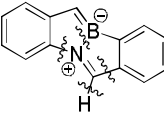
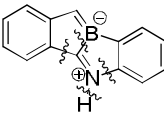
The large gain in energy upon **2,3** \rightarrow **1,3** isomerization is caused solely by the rise in $\Delta\Delta E_{int} = 22.95$ kcal/mol, while deformation energy change is slightly negative ($\Delta\Delta E_{def} = -1.14$

Table 3. Contribution of various energy components to the total binding interactions between three fragments in the studied BN analogues of dibenzopentalene and energy changes (values in bold) occurring upon constitutional isomerization.^[a] Values are in kcal/mol, calculated at the UB3LYP/6-311+G(d,p) level.

Molecule	ΔE_{tot}	ΔE_{def}	ΔE_{int}	ΔE_{elstat}	ΔE_{Pauli}	ΔE_{oi}	ΔE_{disp}	Interacting fragments ^[b]
	ΔE_{iso}	$\Delta\Delta E_{def}$	$\Delta\Delta E_{int}$	$\Delta\Delta E_{elstat}$	$\Delta\Delta E_{Pauli}$	$\Delta\Delta E_{oi}$	$\Delta\Delta E_{disp}$	
 1,4	-490.23	59.71	-549.84	-576.08	1097.20	-953.0	-118.06	H(doublet) CN(sextet) C ₁₃ H ₉ B(quintet)
 3,1	-487.67	64.99	-552.66	-573.91	1106.98	-968.82	-116.91	H(doublet) CN(sextet) C ₁₃ H ₉ B (quintet)
1,4 \rightarrow 3,1	2.56	5.28	-2.72	2.17	9.78	-15.82	1.15	

[a] Labeling of energy terms is the same as in Table 2. [b] Interacting fragments involved in ΔE_{int} energy.

Table 4. Contribution of various energy components to the total binding interactions between three fragments in the studied BN analogues of dibenzopentalene and energy changes (values in bold) occurring upon constitutional isomerization.^[a] Values are in kcal/mol, calculated at the UB3LYP/6-311+G(d,p) level.

Molecule	ΔE_{tot}	ΔE_{def}	ΔE_{int}	ΔE_{elstat}	ΔE_{Pauli}	ΔE_{oi}	ΔE_{disp}	Interacting fragments ^[b]
	ΔE_{iso}	$\Delta \Delta E_{\text{def}}$	$\Delta \Delta E_{\text{int}}$	$\Delta \Delta E_{\text{elstat}}$	$\Delta \Delta E_{\text{Pauli}}$	$\Delta \Delta E_{\text{oi}}$	$\Delta \Delta E_{\text{disp}}$	
 2,3	-496.12	82.28	-578.40	-738.14	1319.39	-1063.77	-95.88	H(doublet) BC ⁻ (quintet) C ₁₃ H ₉ N ⁺ (quartet)
 3,1	-498.21	62.40	-560.61	-356.20	650.58	-735.75	-119.24	H(doublet) BC(sextet) C ₁₃ H ₉ N (quintet)
2,3 → 3,1	-2.09	-19.88	17.79	381.94	-668.81	328.02	-23.36	
 2,3	-629.93	93.83	-723.56	-490.90	904.14	-1040.57	-96.23	H(doublet) CN ⁺ (quintet) C ₁₃ H ₉ B ⁻ (quartet)
 1,3	-607.92	92.69	-700.61	-363.70	861.06	-1101.39	-96.58	H(doublet) CN ⁺ (quintet) C ₁₃ H ₉ B ⁻ (quartet)
2,3 → 1,3	21.81	-1.14	22.95	127.20	-43.08	-60.82	-0.35	

[a] Labeling of energy terms is the same as in Table 2. [b] Interacting fragments involved in ΔE_{int} energy.

kcal/mol). Our analysis in Table 4 shows that there is just one energy component which is more favourable in the more stable **2,3** isomer, electrostatic attraction. This should be primarily related to the larger electrostatic component of the B–N bond in **2,3** vs the B–C bond in **1,3**. In the former, the difference in partial atomic charges is 0.146e and in the latter 0.022e.

Influence of BN pair position on (anti)aromaticity of individual rings, bicycles and molecular perimeter

This section deals with the effect of various arrangements of BN pair within the central butadiene moiety on (anti)aromaticity of individual rings, bicyclic substructures and of molecular perimeter. The calculated aromaticity indices are shown in Figure 7.

We begin with a brief discussion of (anti)aromaticity of the parent hydrocarbon, dibenzopentalene. Annulation of two benzene units with pentalene decreases benzene's aromaticity and reduces antiaromaticity of five-membered rings in pentalene, so that the latter can be considered as nonaromatic, or at most very weakly antiaromatic in dibenzopentalene. Weakly antiaromatic perimeter of pentalene becomes nonaromatic in dibenzopentalene. Benzene-fused five-membered ring moiety in dibenzopentalene can be considered as nonaromatic (HOMA), or weakly aromatic (FLU π), while molecular perimeter is weakly

aromatic. These results are comparable with previous computations.^[15,34]

In BN-dibenzopentalene isomers, benzene rings are more, or less aromatic, except in **1,3** for which NICS(1)_{zz} = 26.7 ppm indicates paratropicity and in **2,3**, where one benzene is magnetically nonaromatic (NICS(1)_{zz} = 4.2 ppm). These results, as well as the large paratropicity of benzene in benzo[c]borole (NICS(1)_{zz} = 102 ppm), were further investigated by the NICS-XY-scan procedure, developed by Stanger and co-workers.^[35] The method provides an insight into the type of ring currents in a molecule (diatropic, paratropic, local, semi-local and global). Calculations were performed by using the Aroma 1.0 package at the B3LYP/6-311+G(d,p) level of theory and scans were obtained at the distance of 1.7 Å from the plane of the molecule. The use of the σ -only model provided only the π -electron contributions, that is the NICS π_{zz} values (Figure S2 in the Supporting Information). The shape of the curves obtained for the 8 π -electron benzo[c]borole and benzo[c]borole moiety in **1,3** isomer resemble the shape of the curve calculated previously for the indenyl cation^[35d] and contain one global maximum centered at the borole ring (100 ppm and 45 ppm, respectively) and one local maximum centered at the benzene ring (57 ppm and 15 ppm, respectively). In the case of the benzo-fused azaborolidine substructure of **2,3** isomer the curve is pretty flat above the benzene ring with NICS values which are around zero and there

is a global maximum above the azaborolidine ring with the value of 20 ppm. These results can be interpreted by the existence of a global paratropic current at the perimeter of benzo[*c*]borole and weaker semilocal paratropic currents at the perimeter of the benzo-fused substructures of **1,3** and **2,3** isomers, which are counteracted by the local diatropic current of benzene ring. Their superposition results in the paratropic effect of benzene in benzo[*c*]borole and weak paratropic effect of benzene in **1,3** isomer. In **2,3** isomer the paratropic currents are the weakest and are canceled by the diatropic currents of benzene resulting in the net NICS values close to zero. Our calculations on benzo[*c*]borole having the same geometry as that in **1,3** isomer, but without having the rest of the molecule (C₆H₅N), indicate extremely high paratropicity: 167.9 ppm for benzene moiety and 314.7 ppm for borole moiety, which should be a consequence of the increased global paratropic ring current. Since both optimized benzo[*c*]borole and benzo[*c*]borole derived from **1,3** isomer contain the six π -electronic benzene ring and the three center two electron bond comprising boron atom and the two neighbouring carbon atoms,^[36] it can be concluded that the charge-separation reduced the paratropic effect of benzo[*c*]borole substructure.

The pattern of BN position within the central butadiene fragment does not affect nonaromaticity of pentalene perimeter to great extent. Thus, it is similarly nonaromatic in **1,2** and **1,4** isomers, as it is in dibenzopentalene and is slightly more delocalized, but still nonaromatic in other four isomers. The ranges of calculated HOMA values (0.484-0.700) and of FLU _{π} values (0.1138-0.2962) point to slight variations in the strength of electron delocalization at molecular perimeter with variations of BN pair position within the central part of molecule. A conclusion based on FLU _{π} index, which is related to only π component of chemical bonds, is that the largest delocalization can be expected for charge separated **2,3** isomer (FLU _{π} = 0.1138) and the smallest for **1,4** isomer (FLU _{π} = 0.2962). They would be more and less delocalized than dibenzopentalene (FLU _{π} = 0.1403). The HOMA data, which are based on both σ and π components of chemical bonds, partly support this conclusion. Thus, HOMA for **2,3** and **1,4** are 0.645 and 0.543, though these are not the highest and the lowest values (Figure 7). This conclusion can be rationalized as follows. The push-pull nature of BN-substituted butadiene fragment in **1,4** enhances internal π -electron delocalization (Figure 9) thereby diminishing delocalization along molecular perimeter. In **2,3**, the π -system is destabilized because of its separated charges. This instability, in turn, drives the π -electron delocalization. In the case of simple, monocyclic azaborine isomers we found the same effects to be responsible for the highest and weakest aromaticity of 1,3- and 1,4-azaborine isomers, respectively.^[12c] According to both indices, another charge-separated **1,3** isomer has smaller peripheral delocalization than **2,3**. This can be ascribed to the existence of 8 π -electron benzo[*c*]borole subunit in **1,3**, the perimeter of which is less delocalized than perimeter of two benzazaborole moieties in **2,3** isomer.

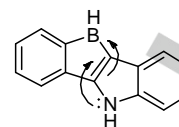


Figure 9. The π -electron delocalization within the central BN-substituted butadiene fragment of **1,4** isomer of dibenzopentalene.

The pattern of BN position, however, greatly affects (anti)aromatic character of five-membered rings and benzene-fused five-membered rings. Thus, when indole subunit is formed (**2,1** and **1,4** isomers) or isoindole (**3,1** isomer), they are aromatic compared to the nonaromatic (HOMA), or weakly aromatic (FLU _{π}) corresponding hydrocarbon moiety of dibenzopentalene. Aromaticity of indole subunit depends on its orientation within the molecule. In **1,4** isomer it is more aromatic than in **2,1** isomer, which possesses the B–N bond. This can be attributed to the partial loss of 10 π -electronic density of indole subunit in **2,1** due to the N \rightarrow B π -electron donation, which acts in opposite direction than nitrogen resonance effect in indole ring. In **1,4** isomer, N \rightarrow B π -electron donation, via the C=C double bond, goes in same direction as its resonance effect in indole ring. The peripheral aromaticity of indole moiety in **1,4** is similar to aromaticity of indole itself. In **3,1** isomer, perimeter of isoindole moiety is similarly aromatic as is the perimeter of isoindole. Benzene rings fused to pyrroles in **2,1** and **1,4** isomers are more aromatic than benzene fused to pyrrole in **3,1** isomer. This is a clear indication of the loss of π -electronic aromatic sextet of benzene in **3,1** which forms the π -neutral structure instead of, otherwise, charge-separated structure. Pyrrole rings in **1,4** and **3,1** isomers are aromatic, but less so than pyrrole itself. Their aromaticity is also weaker (according to HOMA and NICS(1)_{zz}), or slightly larger (according to FLU _{π}) than aromaticity of the respective moieties in indole and isoindole. However, aromaticity of pyrrole ring decreases significantly when nitrogen atom forms the bond with electron-deficient boron atom, as in **2,1** isomer. Here, pyrrole moiety becomes at most weakly aromatic. This, again, is attributable to the partial loss of π -electron density from pyrrole ring due to N \rightarrow B electron donation. In **1,4**, as mentioned, N \rightarrow B π -electron donation goes over the CC double bond of pyrrole ring.

The perimeter of benzo[*b*]borole moieties in **1,2** and **1,4** isomers is nonaromatic to weakly antiaromatic compared with the weakly antiaromatic perimeter of benzo[*b*]borole. It is less delocalized than the perimeter of the corresponding hydrocarbon part of dibenzopentalene, which was assigned as nonaromatic to weakly aromatic. The orientation of the benzo[*b*]borole moiety in a molecule (**1,2** and **1,4** isomers) does not seem to have a profound impact on its peripheral delocalization. According to HOMA and FLU _{π} , the perimeter of benzo[*c*]borole moiety in **1,3** is nonaromatic, similarly as the perimeter of benzo[*c*]borole, and is thus less delocalized than the corresponding hydrocarbon part of dibenzopentalene. Borole rings, which are present in these three isomers, **1,2**, **1,4** and **1,3**, are antiaromatic, but to the lesser extent than borole is.^[37]

The benzene-fused azaborolidine moieties in the charge-separated **2,3** isomer are slightly more delocalized than the corresponding hydrocarbon part of dibenzopentalene. All azaborolidine rings in BN-dibenzopentalenes can be considered as nonaromatic as are the corresponding five-membered rings of the parent dibenzopentalene.

Conclusions

Due to the scarce literature data on BN/CC isosterism in $4n\pi$ -electronic systems we have theoretically studied six isomeric BN analogues of dibenzopentalene. A derivative of one of them has been accessed experimentally.^[16] Emphasis of our investigation was on two fundamental properties: stability and (anti)aromaticity.

Different BN substitution patterns within the central butadiene moiety of dibenzopentalene can widen the energy range between isomers to ~52 kcal/mol. Four isomers have neutral π -electronic system, **1,2**, **2,1** (11.2 kcal/mol), **1,4** (25.2 kcal/mol) and **3,1** (27.8 kcal/mol), and two isomers have charge-separated π -electronic system, **2,3** (29.9 kcal/mol) and **1,3** (51.8 kcal/mol). The latter two are clearly destabilized by charge-separation. Among the BN-orientational isomers (two such pairs, **1,2/2,1** and **1,3/3,1**), more stable one contains the 10π -electron aromatic (iso)indole substructure vs the nonaromatic 8π -electron benzoborole substructure in the less stable isomer. Stability order of BN-orientational isomers follows the order of their local, semilocal and global aromaticity. However, this is not the case for all isomers, so that their relative energies were further examined by bond dissociation energies of B–C, B–N, C–C and C–N bonds and additionally by the isomerization energy decomposition analysis (IEDA) which provided more insight into the factors which are responsible for the observed energy trend.

The **1,4** isomer is destabilized by larger indole-benzene or benzoborole-benzene Pauli repulsion with respect to **2,1** and **1,2** isomers, respectively, and additionally by $N_{LP}-CC_{\pi}$ repulsion relative to **1,2**. Such destabilization is the main factor responsible for higher energy of **1,4** relative to **1,2**, but is significantly counteracted by the more stabilizing orbital interactions of **1,4** relative to **2,1**. Thus, the larger attractive electrostatic component of the BN bond in **2,1** vs the BC bond in **1,4** presents the main source of energy rise when going from **2,1** to **1,4** isomer. Further slight destabilization on going from **1,4** to **3,1** isomer comes solely from structural changes. The **3,1** isomer escapes charge-separation of the π -system of the central butadiene moiety by forming the isoindole substructure. Although **2,3** isomer can not escape from charge-separation, it is only slightly less stable than the preceding member on energy scale (**3,1** isomer). The IEDA revealed that the charge-separation of **2,3** acts in two opposite directions: it destabilizes the π -system relative to the neutral one of **3,1**, but strengthens the electrostatic attractive component of chemical bonds. Another effect contributing to the small energy difference between **2,3** and **3,1** is larger orbital interaction energy in the former. The large energy difference between the two charge-separated **2,3** and **1,3** isomer is caused only by the greater

electrostatic attractive interactions in the former, which was attributed mainly to the B–N bond in **2,3** vs the B–C bond in **1,3**.

Various arrangements of the BN pair within the central butadiene moiety of dibenzopentalene mostly affect aromaticity of five-membered and benzene-fused five-membered subunits containing one heteroatom. Thus, pyrrole moieties are aromatic and borole moieties are antiaromatic compared to the nonaromatic five-membered hydrocarbon moiety of dibenzopentalene. The (iso)indole moieties are aromatic and benzoborole ones are nonaromatic to weakly antiaromatic compared to the nonaromatic and slightly more delocalized hydrocarbon subunit in dibenzopentalene. Orientation of heterocyclic subunits within the molecule affects delocalization of only aromatic ones: when the B–N bond appears aromaticity decreases. Nonaromaticity of azaborolidine and benzazaborolidine subunits mostly compare with that of the corresponding hydrocarbon parts of dibenzopentalene. The net paratropic effect of benzene in **1,3** isomer is interpreted as the superposition of the semi-local paratropic current of benzo[c]borole substructure and local diatropic current of benzene. In all BN-dibenzopentalenes the perimeter of pentalene moiety remains nonaromatic, while molecular periphery is slightly affected by BN pair positions. The π -electron charge-separation in **2,3** drives more peripheral delocalization relative to the parent molecule, while internal N–C=C–B delocalization of **1,4** decreases delocalization at molecular perimeter.

Acknowledgements

This work was supported by the Ministry of Education, Science and Technological Development of the Republic of Serbia, project No. 172020.

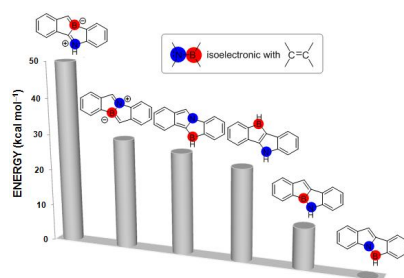
Keywords: boron • density functional calculations • electronic structure • fused-ring systems • nitrogen

- [1] O. T. Summerscales, F. G. N. Cloke, *Coord. Chem. Rev.* **2006**, *250*, 1122-1140.
- [2] T. Cai, L. Xu, C. Shu, J. E. Reid, H. W. Gibson, H. C. Dorn, *J. Phys. Chem. C* **2008**, *112*, 19203-19208.
- [3] H. Hopf, *Angew. Chem. Int. Ed.* **2013**, *52*, 12224-12226; *Angew. Chem.* **2013**, *125*, 12446-12449.
- [4] a) T. Wurm, E. C. Rüdiger, J. Schulmeister, S. Koser, M. Rudolph, F. Rominger, U. H. F. Bunz, A. S. K. *Chem. Eur. J.* **2018**, *24*, 2735-2740; b) D. C. Grenz, M. Schmidt, D. Kratzert, B. Esser, *J. Org. Chem.* **2018**, *83*, 656-663; c) G. Dai, J. Chang, L. Jing, C. Chi, *J. Mater. Chem. C* **2016**, *4*, 8758-8764; d) J.-J. Shen, J.-Y. Shao, X. Zhu, Y.-W. Zhong, *Org. Lett.* **2016**, *18*, 256-259; e) C. Li, C. Liu, Y. Li, X. Zhu, Z. Wang, *Chem. Comm.* **2015**, *51*, 693-696; f) T. Kawase, J.-i. Nishida, *Chem. Rec.* **2015**, *15*, 1045-1059.
- [5] a) H. Oshima, A. Fukuzawa, S. Yamagichu, *Angew. Chem. Int. Ed.* **2017**, *56*, 3270-3274; *Angew. Chem.* **2017**, *129*, 3318-3322; b) C. K. Frederickson, L. N. Zakharov, M. M. Haley, *J. Am. Chem. Soc.* **2016**, *138*, 16827-16838.
- [6] M. Saito, *Symmetry* **2010**, *2*, 950-969.
- [7] A. Konishi, Y. Okada, M. Nakano, K. Sugisaki, K. Sato, T. Takui, M. Yasuda, *J. Am. Chem. Soc.* **2017**, *139*, 15284-15287.

- [8] For reviews, see: a) Z. X. Giustra, S.-Y. Liu, *J. Am. Chem. Soc.* **2018**, *140*, 1184-1194; b) G. Bélanger-Chabot, H. Braunschweig, D. K. Roy, *Eur. J. Inorg. Chem.* **2017**, 4353-4368; c) H. Helten, *Chem. Eur. J.* **2016**, *22*, 12972-12982; d) X. Y. Wang, J.-Y. Wang, J. Pei, *Chem. Eur. J.* **2015**, *21*, 3528-3539; e) P. G. Campbell, A. J. V. Marwitz, S.-Y. Liu, *Angew. Chem. Int. Ed.* **2012**, *51*, 6074-6092; *Angew. Chem.* **2012**, *124*, 6178-6197; f) M. J. D. Bosdet, W. E. Piers, *Can. J. Chem.* **2009**, *87*, 8-29; g) Z. Liu, T. B. Marder, *Angew. Chem. Int. Ed.* **2008**, *47*, 242-244; *Angew. Chem.* **2007**, *120*, 248-250.
- [9] a) T. Lorenz, M. Crumbach, T. Eckert, A. Lik, H. Helten, *Angew. Chem. Int. Ed.* **2017**, *56*, 2780-2784; *Angew. Chem.* **2017**, *129*, 2824-2828; b) Z. Zhong, X.-Y. Wang, F.-D. Zhuang, N. Ai, J. Wang, J.-Y. Wang, J. Pei, J. Peng, Y. Cao, *J. Mater. Chem. A* **2016**, *4*, 15420-15425; c) J.-Y. Wang, J. Pei, *Chinese Chem. Lett.* **2016**, *27*, 1139-1146.
- [10] a) A. Vlasceanu, M. Jessing, J. P. Kilburn, *Bioorg. Med. Chem.* **2015**, *23*, 4453-4461; b) D. H. Knack, J. L. Marshall, G. P. Harlow, A. Dudzik, M. Szaleniec, S.-Y. Liu, J. Heider, *Angew. Chem. Int. Ed.* **2013**, *52*, 2599-2601; *Angew. Chem.* **2013**, *125*, 2660-2662.
- [11] S. Xu, Y. Zhang, B. Li, S.-Y. Liu, *J. Am. Chem. Soc.* **2016**, *138*, 14566-14569.
- [12] a) J. S. A. Ishibashi, A. Dargelos, C. Darrigan, A. Chrostowska, S.-Y. Liu, *Organometallics* **2017**, *36*, 2494-2497; b) Z. Liu, J. S. A. Ishibashi, C. Darrigan, A. Dargelos, A. Chrostowska, B. Li, M. Vasiliiu, D. A. Dixon, S.-Y. Liu, *J. Am. Chem. Soc.* **2017**, *139*, 6082-6085; c) M. Baranac-Stojanović, *Chem. Eur. J.* **2014**, *20*, 16558-16565; d) A. Chrostowska, S. Xu, A. N. Lamm, A. Mazière, C. D. Weber, A. Dargelos, P. Baylère, A. Graciaa, S.-Y. Liu, *J. Am. Chem. Soc.* **2012**, *134*, 10279-10285; e) D. Ghosh, G. Periyasamy, S. K. Pati, *Phys. Chem. Chem. Phys.* **2011**, *13*, 20627-20636; f) E. R. Abbey, L. N. Zakharov, S.-Y. Liu, *J. Am. Chem. Soc.* **2008**, *130*, 7250-7252.
- [13] C. Ma, J. Zhang, J. Li, C. Cui, *Chem. Comm.* **2015**, *51*, 5732-5734.
- [14] X.-Y. Wang, A. Narita, X. Feng, K. Müllen, *J. Am. Chem. Soc.* **2015**, *137*, 7668-7671.
- [15] M. Dimitrova, H. Filegl, D. Sundholm, *Phys. Chem. Chem. Phys.* **2017**, *19*, 20213-20223.
- [16] A. Iida, A. Sekioka, S. Yamaguchi, *Chem. Sci.* **2012**, *3*, 1461-1466.
- [17] a) A. D. Becke, *J. Chem. Phys.* **1993**, *98*, 5648-5652; b) C. Lee, W. Yang, R. G. Parr, *Phys. Rev. B: Condens. Matter Mater. Phys.* **1988**, *37*, 785-789; c) J. B. Foresman, A. Frisch in *Exploring Chemistry with Electronic Structure Methods*, Gaussian, Inc., **1996**.
- [18] M. J. Frisch, G. W. Trucks, H. B. Schlegel, G. E. Scuseria, M. A. Robb, J. R. Cheeseman, G. Scalmani, V. Barone, B. Mennucci, G. A. Petersson, H. Nakatsuji, M. Caricato, X. Li, H. P. Hratchian, A. F. Izmaylov, J. Bloino, G. Zheng, J. L. Sonnenberg, M. Hada, M. Ehara, K. Toyota, R. Fukuda, J. Hasegawa, M. Ishida, T. Nakajima, Y. Honda, O. Kitao, H. Nakai, T. Vreven, J. A. Montgomery, Jr., J. E. Peralta, F. Ogliaro, M. Bearpark, J. J. Heyd, E. Brothers, K. N. Kudin, V. N. Staroverov, T. Keith, R. Kobayashi, J. Normand, K. Raghavachari, A. Rendell, J. C. Burant, S. S. Iyengar, J. Tomasi, M. Cossi, N. Rega, J. M. Millam, M. Klene, J. E. Knox, J. B. Cross, V. Bakken, C. Adamo, J. Jaramillo, R. Gomperts, R. E. Stratmann, O. Yazyev, A. J. Austin, R. Cammi, C. Pomelli, J. W. Ochterski, R. L. Martin, K. Morokuma, V. G. Zakrzewski, G. A. Voth, P. Salvador, J. J. Dannenberg, S. Dapprich, A. D. Daniels, O. Farkas, J. B. Foresman, J. V. Ortiz, J. Cioslowski, D. J. Fox, *Gaussian 09 (Revision D.01)*, Gaussian, Inc., Wallingford CT, 2013.
- [19] a) T. M. Krygowski, H. Szatylowicz, O. A. Stasyuk, J. Dominikowska, M. Palusiak, *Chem. Rev.* **2014**, *114*, 6383-6422; b) T. M. Krygowski, M. K. Cyrański, *Chem. Rev.* **2001**, *101*, 1385-1419; c) J. Kruszewski, T. M. Krygowski, *Tetrahedron Lett.* **1972**, 3839-3842.
- [20] E. Matito, M. Duran, M. Solà, *J. Chem. Phys.* **2005**, *122*, 014109.
- [21] H. Fallah-Bagher-Shaidaei, C. S. Wannere, C. Corninboeuf, R. Puchta, P. v. R. Schleyer, *Org. Lett.* **2006**, *8*, 863-866.
- [22] T. Lu, F. Chen, *J. Comput. Chem.* **2012**, *33*, 580-592.
- [23] a) R. Ditchfield, *Mol. Phys.* **1974**, *27*, 789-807; b) K. Wolinski, J. F. Hinton, P. Pulay, *J. Am. Chem. Soc.* **1990**, *112*, 8251-8260.
- [24] P. Su, H. Li, *J. Chem. Phys.* **2009**, *131*, 014102.
- [25] M. W. Schmidt, K. K. Baldrige, J. A. Boatz, S. T. Elbert, M. S. Gordon, J. H. Jensen, S. Koseki, N. Matsunaga, K. A. Nguyen, S. J. Su, T. L. Windus, M. Dupuis, J. A. Montgomery, Jr., *J. Comput. Chem.* **1993**, *14*, 1347-1363; Gamess 2013-R1 version was used.
- [26] The energy trend of BN-substituted *trans*-butadienes obtained in this work is in full accordance with the one which was obtained previously at the CCSD(T)/6-311G(d,p)//M06-2X/6-311G(d,p) level of theory. See, A. M. Rouf, J. Wu, J. Zhu, *Chem. Asian J.* **2017**, *12*, 605-614.
- [27] If there was a slight diradical state, spin density would be distributed over the benzo[*c*]borole moiety, mostly at C3 and C2/B atoms (Table S2 in the Supporting Information).
- [28] F. L. Hirshfeld, *Theor. Chim. Acta.* **1977**, *44*, 129-138.
- [29] a) M. H. Matus, S.-Y. Liu, D. A. Dixon, *J. Phys. Chem. A* **2010**, *114*, 2644-2654; b) J. E. Del Bene, M. Yáñez, I. Alkorta, J. Elguero, *J. Chem. Theory Comput.* **2009**, *5*, 2239-2247; c) M. Kranz, T. Clark, *J. Org. Chem.* **1992**, *57*, 5492-5500.
- [30] M. Baranac-Stojanović, *Eur. J. Org. Chem.* **2017**, 5163-5169.
- [31] D. J. Grant, D. A. Dixon, *J. Phys. Chem. A* **2006**, *110*, 12955-12962.
- [32] We wish to point out that isomerization energy decomposition analysis was used previously to study the origin of the preferred geometry of various species: a) M. Contreras, E. Osorio, F. Ferraro, G. Puga, K. J. Donald, J. G. Harrison, G. Merino, W. Tiznado, *Chem. Eur. J.* **2013**, *19*, 2305-2310; b) E. Ravell, S. Jalife, J. Barroso, M. Orozco-Ic, G. Hernández-Juárez, F. Ortiz-Chi, S. Pan, J. L. Cabellos, G. Merino, *Chem. Asian J.* **2018**, *13*, 1467-1473; c) A. Vásquez-Espinal, K. Palacio-Rodríguez, E. Ravell, M. Orozco-Ic, J. Barroso, S. Pan, W. Tiznado, G. Merino, *Chem. Asian J.* **2018**, *13*, 1751-1755; d) X. Dong, S. Jalife, A. Vásquez-Espinal, E. Ravell, S. Pan, J. L. Cabellos, W.-y. Liang, Z.-h. Cui, G. Merino, *Angew. Chem. Int. Ed.* **2018**, *57*, 4627-4631; *Angew. Chem.* **2018**, *130*, 4717-4721, or to rationalize stability trend of some (anti)aromatic compounds: a) M. El-Hamdi, W. Tiznado, J. Poater, M. Solà, *J. Org. Chem.* **2011**, *76*, 8913-8921; b) J. Poater, R. Visser, M. Solà, F. M. Bickelhaupt, *J. Org. Chem.* **2007**, *72*, 1134-1142; (c) references 12c and 30 in this work.
- [33] Z. Džambaski, M. Baranac-Stojanović, *ChemistrySelect* **2017**, *2*, 42-50.
- [34] R. Ayub, O. El Bakouri, K. Jorner, M. Solà, H. Ottosson, *J. Org. Chem.* **2017**, *82*, 6237-6340.
- [35] a) A. Rahalkar, A. Stanger, *Aroma*. <http://chemistry.technion.ac.il/members/amnon-stanger/>; b) A. Stanger, *J. Org. Chem.* **2006**, *71*, 883-893; c) A. Stanger, *J. Org. Chem.* **2010**, *75*, 2281-2288; d) R. Gershoni-Poranne, A. Stanger, *Chem. Eur. J.* **2014**, *20*, 5673-5688.
- [36] This was deduced on the basis of natural bond orbitals (NBO) analysis, done with the NBO 6.0 linked to the Gaussian 09: a) E. D. Glendening, J. K. Badenhoop, A. E. Reed, J. E. Carpenter, J. A. Bohmann, C. M. Morales, C. R. Landis, F. Weinhold, NBO 6.0, Theoretical Chemistry Institute, University of Wisconsin, Madison, WI, 2013; b) E. D. Glendening, C. R. Landis, F. Weinhold, *WIREs Comput. Mol. Sci.* **2012**, *2*, 1-42; c) F. Weinhold, C. R. Landis, in *Discovering Chemistry with Natural Bond Orbitals*, John Wiley & Sons, Inc., **2012**.
- [37] Substituent effects on (anti)aromaticity of neutral and anionic borole rings have been studied in ref.: J. O. C. Jimenez-Halla, E. Matito, M. Solà, H. Braunschweig, C. Hörl, I. Krummenacher, J. Wahler, *Dalton Trans.* **2015**, *44*, 6740-6747.

FULL PAPER

The BN/CC isosterism is increasingly exploited to tune physical and biochemical properties of organic compounds. Here, we use density functional calculations to explore how BN/CC substitution modifies local, semi-local and global (anti)aromaticity of the $4n\pi$ -electronic dibenzo[*a,e*]pentalene and to predict and explain relative stability of the six isomeric BN-dibenzo[*a,e*]pentalenes.



Milovan Stojanović, Marija Baranac-Stojanović*

Page No. – Page No.

Analysis of Stability and (Anti)aromaticity of BN-Dibenzo[*a,e*]pentalenes